IABSE-JSCE Joint Conference on Advances in Bridge Engineering-IV, August 26-27, 2020, Dhaka, Bangladesh
Amin, Okui, Bhuiyan, Rahman (eds.)
ISBN: 978-984-34-8313-3
www.iabse-bd.org

Damage evaluation of concrete NWAB girders subjected to torsional loading

Z. Saleheen, S.M. Reza & M.A. Sobhan
Design Planning & Management Consultants Ltd, Dhaka 1205, Bangladesh

R.R. Krishnamoorthy
Smart Manufacturing Research Institute, Universiti Teknologi MARA(UiTM),40450, Shah Alam, Selangor, Malaysia

ABSTRACT: Torsion in concrete was considered as a secondary effect in concrete structures for a long time, thus resulting in uneconomic and impractical design due to torsion. However recent structural codes have implemented design strategies for beams and columns subjected to torsion. Now-a-days Arch bridges are becoming very popular in Bangladesh. While designing arch bridges, the authors realized that due to the geometric configuration of an arch bridge, long girders are subjected to substantial amount of torsion which plays a vital role in selecting member size and reinforcement of the girder. This paper evaluates the damages in reinforced concrete girders by using Abaqus to conduct a nonlinear finite element analysis of RC girders subjected to torsion combined with axial force, shear and bending. Confining reinforcement and longitudinal rebars in the girder were provided using the conventional codes for structural design and then a parametric study was conducted to evaluate the damage on concrete in terms of cracks.

1 INTRODUCTION

Network Arch Bridges (NWAB) are arch bridges which have inclined hangers connecting the arch and long girder therefore transferring the load from deck system to the arch. In order to classify a bridge with inclined hangers as a network arch, the hangers have to cross each other at least twice. During 1955 as a part of his master's Thesis, Norwegian Professor Per Tveit was showing design calculations for Nielsen Bridges and he realized that if the hangers were to cross each other many times, bending in the Arch and Girders could be reduced significantly which will in turn save 75% reinforcements of conventional arch bridges and thus he came up with the idea of NWAB (Tveit, 2006). NWABs can be made of either concrete or steel. Arch bridges in Bangladesh dates back as early as 1920 and yet rather than conventional use of Steel as Arch and Girders material, most of the Arch bridges in Bangladesh was made of concrete arch and deck subsystem in order to keep the maintenance cost low and avoid corrosion degradation (Sobhan, 2015).Upon the first successful implementation of Rayer Bazar Graveyard NWAB in April 2015, NWAB has gained popularity among the Engineers of Bangladesh due to its aesthetically pleasing structural configuration and economic cutbacks from conventional RCC and Prestressed Bridges. However, NWAB has some challenges of its own. While designing NWABs for the last couple of years, the authors realized that because of monolithic casting of slab-cross girder-long girder, the weight from slab and cross girder along with asymmetric traffic loading on the bridge can generate a significant amount of Torsion in the Long Girders. While investigating the structural stability of Steel NWABs, Morais (2013) showed that welded joint between Rib(cross girder) and Tie(long girder) introduces substantial torsional stress in the tie, which is consistent with the authors findings of Concrete NWABs. Therefore, this paper intends to investigate the effects of torsion combined with Shear, Flexure and Axial force due to prestressing on a RC NWAB girder by performing a Static-Nonlinear analysis in commercial FEA software Abaqus CAE version 6.14

Nylander (1945) was among the firsts to investigate torsion in Sweden, he carried out the tests for combined flexure, shear and torsion in rectangular and T sections of concrete without transverse reinforcement. He found out that bending significantly reduces torsional capacity of concrete and theory of plasticity represents the torsional behavior of concrete better than theory of elasticity. His work on torsion had a momentous impact on Swedish codes and thereafter theory of plasticity was used as a basis of torsional calculations. Earliest description of failure modes for torsion was given by Fisher (1968), later on, Lennart Elfgren introduced failure mechanism for combined shear, flexure and torsion at 1972in his doctoral thesis, in which reinforcement yields before concrete compressive failure (Elfgren, 2009).Recently, Rahal & Collins (1995) proposed a three dimensional truss model using Modified Compression Field Theory (MCFT) which was capable of predicting the behavior of rectangular prestressed and reinforced concrete girders with reasonable accuracy for complex combinations biaxial shear, axial force, biaxial bending and torsion. Compatibility of curvature was introduced in this model which allows a better representation of nonlinear shear-torsion interaction diagram, that was found to be on very good agreement with experimental results. Subsequently, calculations for combined bending and torsion of this model was compared with a commercial FE package called SPARCS and Experimental Test results, which were in very good agreement with each other (Rahal & Collins, 2003a).

Current Structural codes have also included the combined effect of torsion-shear-bending by using different methods. ACI 318-11 takes into account for the effect of combined bending and shear by incorporating the equation in clause 11.5.3.7foradditional longitudinal reinforcement. Canadian and AASHTO LRFD code has incorporated an alternative shear and torsion design calculations based on the equations of MCFT to predict the combined effect. Rahal & Collins (2003b) conducted an experimental study on four large reinforced concrete members to evaluate the design provisions of ACI 318-02 and AASHTO LRFD codes. It was found that in ACI code using the recommended value for angle of the inclined compression strut, θ=45° results in highly conservative design and using the lowest permitted value of θ=30° has shown inconsistent results which may lead to an non-conservative design. However, using the MCFT equations in AASHTO lead to value of θ=36°, which gave a reasonably accurate approximations of strength.

Using Finite Element tools to predict the behavior of concrete members subjected to combined axial-shear-flexure-torsion has gained immense popularity over the last few years due to its accurate representation of concrete response under a wide variety of complex loading scenarios. Mostofinejad & Talaeitaba (2011)performed a nonlinear analysis of concrete hollow box, rectangular and T sections subjected to torsion by adopting the smeared crack model of finite element software ANSYS and compared the results with existing experimental test specimens. The fourteen samples were subjected to monotonic torsional loading up to failure. Torsional capacity of the beams was found to be reasonably accurate when compared with the experimental results. It was also shown that smeared cracking model of ANSYS give more precise torsional capacity than ACI 318. Torsional crack pattern and cracking trends showed fine coherence with experimental cracks. However, reduced torsional stiffness in the post cracking zone were a bit dissimilar from the experimental values due to strict sensitivity of the smeared cracks, which resulted in reduced torsional rotation than the experiments. Mondal & Prakash (2015) studied combined effects of torsion and axial force by conducting nonlinear analysis of RC bridge columns. Concrete damage plasticity model of Abaqus Explicit was chosen as the finite element tool for this study. This study showed that CDP model can anticipate the response of concrete under such loading with reasonable accuracy. Moreover, Effect of cross-sectional shape and increased transverse reinforcement ratio on the torsional capacity of rectangular and circular columns were thoroughly investigated in this study.

2 NETWORK ARCH BRIDGE GEOMETRY

The bridge chosen for this study is a 90m span, 4 Lane Highway bridge over Turag river, which is currently being designed by the authors.

Figure 1. 3D view of 90m span NWAB.

Figure 1, the bridge consists of four 3.65m wide traffic lane, 3 arch and girder subsystems with 3 network of hangers connecting those and two 1.5m wide pedestrian walkway at either side of the bridge. Total width of the bridge is 22.1m. The rise of the arches were kept as around 18.5 percent of span of the bridge due to aesthetic reasons. The middle girder also acts as a divider for opposite moving vehicle of traffic lanes. The Arch and deck subsystems were designed as C40 grade concrete.

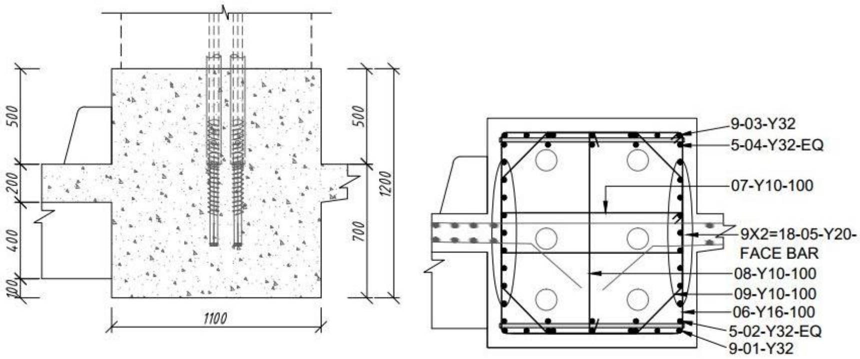

Figure 2. Cross sectional view of the girders.

As shown in Figure 2, the girders are 1100mm X 1200mm, with 16mm closed stirrup spaced at 100mm center to center distance along the girder, 14 numbers of 32mm bars are provided at top and bottom of the girders, and 9 Nos of 20mm bar is provided at each face of the girder. In order to minimize the thrust from arch, all of the girders were post tensioned with 6 Nos of 19K15 prestressing cable of 1860MPa strength. Network Arch Superstructure of the bridge sits on the pier through high damping elastomeric rubber bearing, which allows the bridge to translate in the longitudinal and transverse direction.

3 PARAMETERS USED FOR FINITE ELEMENT MODELLING

3.1 *Loading and Boundary Condition*

Due to the complexity of material nonlinear behavior and it's time consuming nature, modeling was done in two steps. At first the complete bridge superstructure as shown in Figure 1, was modeled using a FE software Midas Civil and all dead loads, pedestrian load, wind load and HL-93 moving load was applied on the model in accordance to AASHTO (2017). After performing analysis in Midas Civil, sectional forces in the girder was taken in service load combination of AASHTO LRFD 2017, which are shown in Table 1.

Then in the next step, a segment of the bridge girder was modeled as 3D continuum solid element in Abaqus CAE. Where one end of the girder was kept fixed and the other end was made free. In the free end of the girder, torsion, axial force and the shear as a downward force was applied to generate desired shear force and moment of Table 1.

Table 1. Resultant forces in girder from step-1.

Beam Force/Moment	
Torsion	770 KN-m
Shear Force	1194 KN
Bending Moment	3343 KN-m
Axial Force	3262 KN

3.2 *Concrete Damage Plasticity Model*

Proper reinforced concrete model should be capable of representing the elastic and plastic behavior of concrete in both compression and tension. Out of three models for concrete, Concrete Damage Plasticity (CDP) model was chosen to model the nonlinear behavior of concrete in both tension and compression. CDP model is based on isotropic damaged elasticity in collaboration of isotropic compressive and tensile plasticity to characterize inelastic performance of concrete. The two failure modes for this plasticity based continuum damage model of concrete are namely tensile cracking and compressive crushing of concrete material (Simulia, 2013). The CDP model is based on the yield function of Lubliner et al. (1989) which was later modified by Lee & Fenves'(1998) assumption of non-associated plastic flow of Drucker-Prager Strength Hypotheses. As shown in Figure 3, concrete behaves as a fully elastic material up to σ_{co} and σ_{to} for compression and tension respectively, beyond that point the plastic region for compression starts with a strain hardening branch up until σ_{cu}, followed by the strain softening region. While for tension, σ_{to} sets off onset micro-cracking in the material, which is embodied by the strain softening branch. Stiffness degradation of concrete during the strain softening branch is designated by a scalar damage variable d_c and d_t for compression and tension respectively(Simulia, 2013).

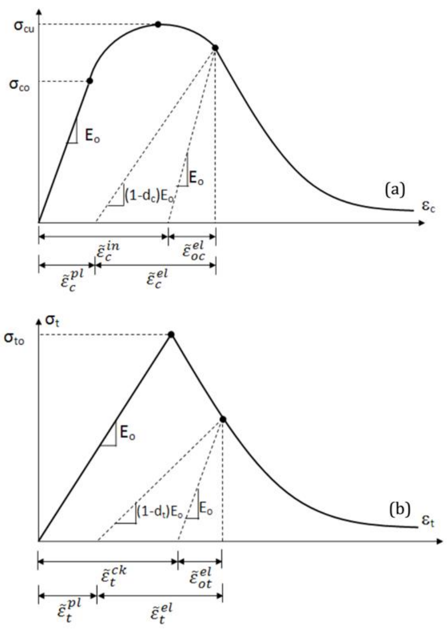

Figure 3. (a) Uniaxial compressive and (b) Uniaxial tensile performance of concrete.

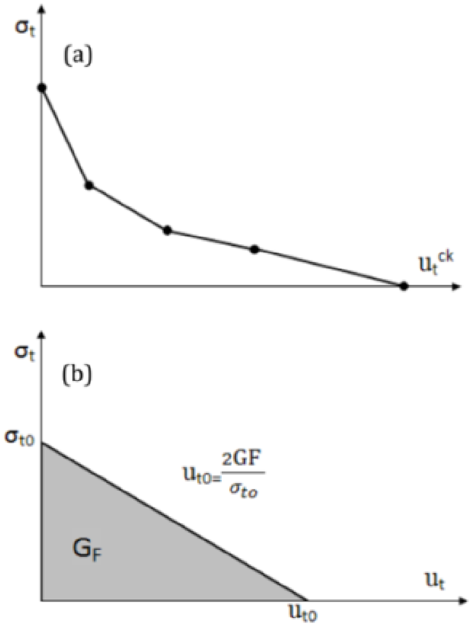

Figure 4. (a) Post failure stress vs. displacement (b) Post failure stress vs. energy curve.

Post failure behavior of concrete can be modeled with tension stiffening, which takes into account for concrete-reinforcement interaction. Tension stiffening for this study was defined using Hillerborg's (1976) cracking energy criteria. As shown in Figure 4, rather than defining post failure stress strain curve, Hillerborg defined tension stiffening using brittle crack concept. He defined the fracture energy required to open a unit area of crack as a material parameter of concrete along with stress displacement relationship to characterize the a brittle behavior of concrete, in order to reduce mesh sensitivity in the model (Hillerborg et al., 1976).Consequently, CEB-FIP (2010) model for 40 MPa concrete using Hillerborg's(1976) cracking energy criterion was adopted as the CDP model for this study.

4 FE MODELLING IN ABAQUS

Modeling the whole NWAB superstructure in Abaqus can be very tedious. For a FE software like Abaqus, analysis time depends on the number of elements or integration points, method of analysis, type of elements etc. As this study aims to evaluate the effects of torsion in Girder only, a 2.8m segment of the girder was chosen as the subject for analysis. Three Static-Nonlinear Analysis was performed for this study to evaluate damage in concrete due to combined shear, torsion, axial force and bending. Loading description for the three models is shown in Table 2.In*ModelT*, only torsional moment was applied to assess the effects of pure torsion in the girder. *Model SMA* was performed to see the effects of all loads except torsion. Finally, analysis of *Model STMA* was performed to observe the effect of torsion combined with axial force, bending and shear.

Table 2. Details of Abaqus FE models.

Model ID	Applied Load	Unit
Model T	Torsion=770	KN, m
Model SMA	Shear=1194+Bending=3343+Axial Force=3262	KN, m
Model STMA	Shear=1194+ Torsion=770 +Bending=3343+Axial Force=3262	KN, m

The concrete girder was modeled as three-dimensional, eight node, hexahedral brick element C3D8R.Stirrups, face bars and longitudinal Reinforcements were modeled as a two-node, linear 3D truss element T3D2. DOF of the reinforcements were kept same as the adjacent girder node by designating reinforcements as embedded elements inside host girder element. The assembled view of concrete girder and steel reinforcements is shown in Figure. Newton's iterative method in Abaqus was used to solve the equilibrium equations for nonlinear analysis of all three models.

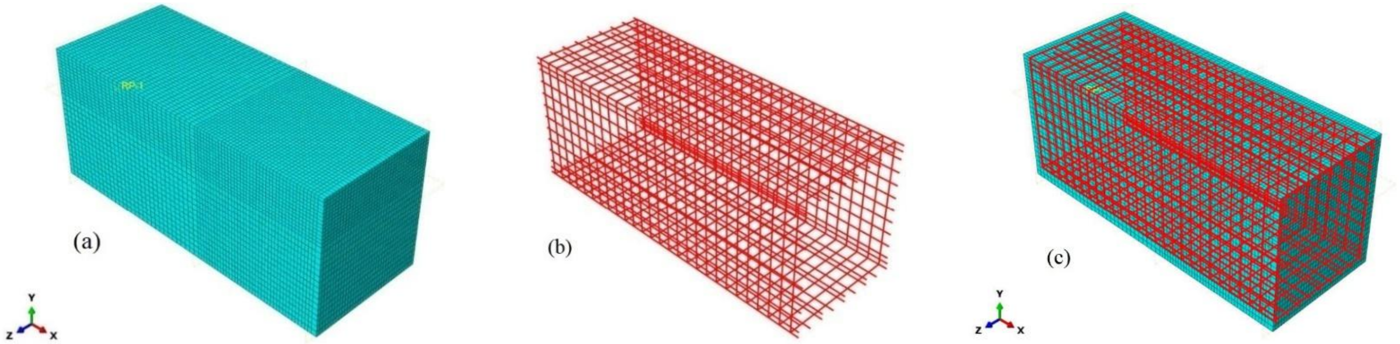

Figure 5. FE model of (a) concrete girder (b) reinforcement (c) assembled girder and reinforcement.

5 RESULTS & DISCUSSIONS

Results of a aforementioned three models namely, *Model T*, *Model SMA* and *Model STMA* will be discussed in this section. Figure shows stress contours for *Model T*. When the girder is subjected to pure torsion (*Model T*), tensile stress develops at the faces of the girder (top, bottom and side) and compressive stresses develops around the sharp angular edges of the girder due to torsion. The stress patterns of *Model T* were found consistent with Jabbar et al. (2016). The Maximum von Mises stress of the girder is 3.96 MPa, which is at side face of girder. For that reason, it can be seen that concrete at the side face and top/bottom face of the girder has reached plastic limit state. Subsequently, Figure shows that a little portion of the girder side and bottom face has lost around 0.367% of its initial material stiffness. However, *Model T* showed no visible crack pattern or major damage in concrete girder due to pure torsion.

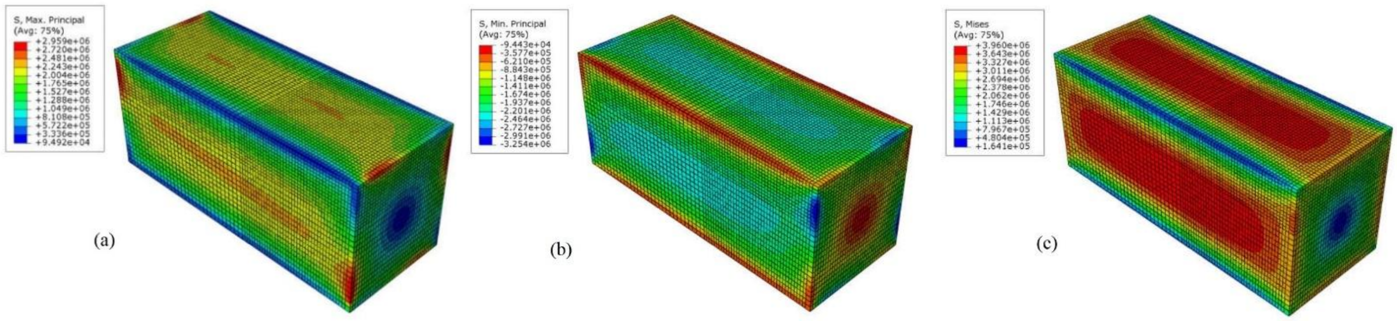

Figure 6.(a) Maximum principal stress. (b) Minimum principal stress. (c) Von Mises Stress, of *Model T*.

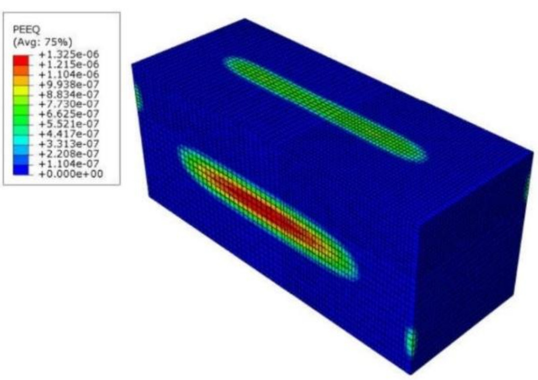

Figure 7. Equivalent plastic strain for *Model T*.

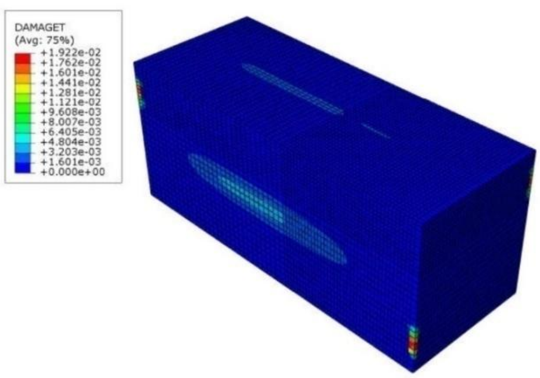

Figure 8. Tensile damage of girder for *Model T*.

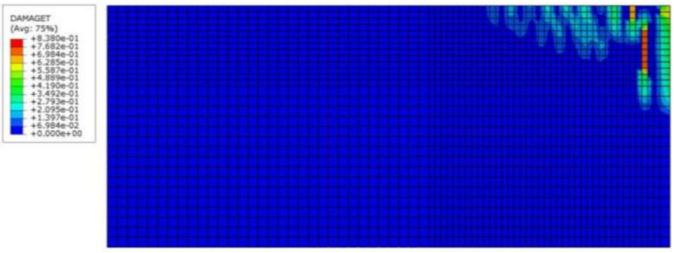

Figure 9. Crack patterns of girder for *Model SMA* (Side Elevation)

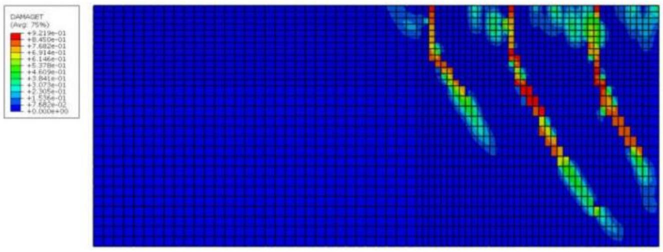

Figure 10. Crack patterns of girder for *Model STMA* (Side Elevation)

In Abaqus, damage of concrete can either happen due to crushing under compression or tension cracking. No damage due to compressive crushing was observed in any of the three models. DAMAGET represents the damage of concrete due to tensile cracking. The range of DAMAGET in Abaqus is between 0 and 1. Value of 0 represents no damage in concrete and 1 indicates in total degradation of material stiffness due to cracking. Figure, Figure and Figure shows crack patterns i.e. tensile damage of concrete in *Model T*, *Model SMA* and *Model STMA* respectively. As mentioned earlier, no visible cracks were observed in *Model T*.

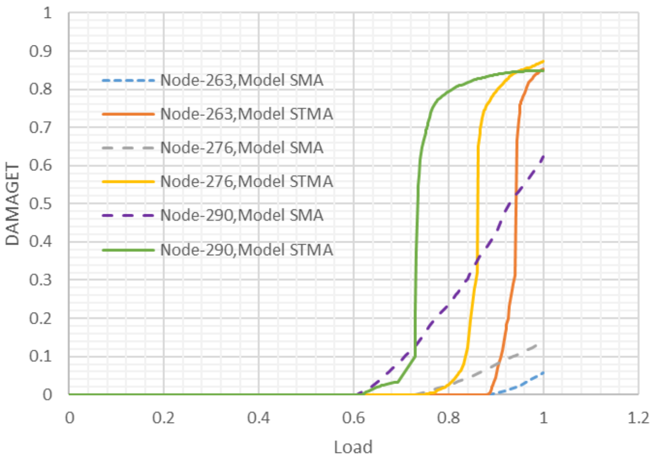

Figure 11. Damage progression rate in girder.

However, *Model SMA* showed up to 85% of tensile damage in concrete, two visible flexure cracks were observed between 100mm to 200mm distance from the end of the girder. Thereafter, until 800mm from the end of the girder, a few minor shear cracks were observed in the model. On the contrary, *Model STMA* showed 3 very prominent cracks at 300mm, 700mm and 1100mm from the end of the girder. Those cracks started off as straight flexural crack then while propagating through the girder they became inclined shear cracks. Apart from these three combined flexure and shear cracks a few minor cracks were also observed at the top of the girder. Node 263, Node 276 and Node 290 are located at top left edge of the girder from 300mm, 700mm and 1100mm distance to the end of the girder respectively. Figure 11 shows the damage progression rate of those nodes. The range of horizontal axis value is between 0 and 1. 0 represents 0% of total applied load and 1 indicates 100% of total applied load. Vertical axis represents the tensile scalar damage variable DAMAGET. At 300mm from end of the girder, tension cracking starts at around 90% of total load of girder and it goes to 5% and 85% damage at full load for *Model SMA* and *Model STMA* respectively. Whilst, at 700 mm from end of the girder, damage starts off at 75% of total load and reaches up to 15% and 87% damage at full load for *Model SMA* and Model *STMA* respectively. Contrarily, at 1100mm from end of the girder, damage for *Model SMA* reaches up to 60% of total damage at full load and 85% for *Model STMA*.

6 CONCLUSIONS

The authors have concluded this study with two prime findings. Firstly, the magnitude of torsion that occurs in the girder didn't have any notable effects on the girder by itself. When the Girder was subjected to only torsion, no visible cracks were observed in the model, only a very insignificant amount of damage occurred in the girder due to pure torsion. On the contrary, this magnitude of torsion along with axial force, bending and shear can generate significant cracking outside the confined reinforcement zone of the girder. Secondly, the prominent cracks due combined axial, flexure, shear and torsion were observed at zones with high shear and torsion. Although, at flexural region of the girder, damage in concrete was increased slightly after the incursion of torsional moment, major torsional damage was observed beyond the flexural region, at near regions where shear force and torsion were both at their zenith. Therefore, the cracks appeared at that region was observed to start off as flexural crack then transforming into inclined shear cracks. Even though the FE model developed for this study is capable of showing the crack patterns, material degradation and redistribution of stresses after cracking very clearly, crack widths cannot be envisioned at this stage of analysis. An extended finite element study (XFEM) needs to conducted to achieve that output. Finally, based on the findings of this study, the authors would like to recommend the practicing structural designers to conduct a comprehensive nonlinear analysis for structures where combined actions of Axial, Shear, Flexure and Torsion are likely to occur.

REFERENCES

AASHTO. (2017). *AASHTO LRFD Bridge Design Specifications*. Washington, DC : American Association of State Highway and Transportation Officials, [©2017].

CEB-FIP. (2010). *fib Model Code for Concrete Structures*.

Elfgren, L. (2009). Development of Models for Torsion of Concrete Structures in Northern Europe. *ACI Symposium Publication*, *265*, 309–326. https://doi.org/10.14359/51663301

Fisher, G. P. (Editor). (1968). Torsion of Structural Concrete. *Special Publication No 18, American Concrete Institute*, 505pp.

Hillerborg, A., Modéer, M., & Petersson, P. E. (1976). Analysis of Crack Formation and Crack Growth in Concrete by Means of Fracture Mechanics and Finite Elements. *Cement and Concrete Research*, *6*, 773–781. https://doi.org/10.1016/0008-8846(76)90007-7

Jabbar, S., Hejazi, F., & Mahmod, H. M. (2016). Effect of an Opening on Reinforced Concrete Hollow Beam Web under Torsional, flexural and Cyclic Loadings. *Latin American Journal of Solids and Structures*, *13*(8), 1576–1595. https://doi.org/10.1590/1679-782512629

Lee, J., & Fenves, G. L. (1998). Plastic Damage Model for Cyclic Loading of Concrete Structures. *Journal of Engineering Mechanics*, *124*(8), 892–900.

Lubliner, J., Oliver, J., Oller, S., & Onate, E. (1989). A Plastic-Damage Model. *International Journal of Solids and Structures*, *25*(3), 299–326.

Mondal, T. G., & Prakash, S. S. (2015). Nonlinear Finite-Element Analysis of RC Bridge Columns under Torsion with and without Axial Compression. *Journal of Bridge Engineering*, *21*(2), 1–13. https://doi.org/10.1061/(ASCE)BE.1943-5592.0000798

Morais, B. (2013). *Design and Analysis of a Network Arch Bridge*.

Mostofinejad, D., & Talaeitaba, S. B. (2011). Nonlinear Modeling of RC Beams Subjected to Torsion using the Smeared Crack Model. *The Twelfth East Asia-Pacific Conference on Structural Engineering and Construction*, *14*, 1447–1454. https://doi.org/10.1016/j.proeng.2011.07.182

Nylander, H. S. E. (1945). *Torsion and Torsional Restraint by Concrete Structures*. Statens Kommittee för Byggnadsforskning, Stockholm, Sweden.

Rahal, K. N., & Collins, M. P. (1995). Analysis of Sections Subjected to Combined Shear and Torsion - A Theoretical Model. *ACI Materials Journal*, *92*(4), 459–469. https://doi.org/10.14359/995

Rahal, K. N., & Collins, M. P. (2003a). Combined Torsion and Bending in Reinforced and Prestressed Concrete Beams. *ACI Structural Journal*, *100*(2), 157–165.

Rahal, K. N., & Collins, M. P. (2003b). Experimental evaluation of ACI and AASHTO-LRFD design provisions for combined shear and torsion. *ACI Structural Journal*, *100*(3), 277–282. https://doi.org/10.14359/12601

Simulia. (2013). ABAQUS Version 6.14, User Manual. Retrieved from Dassault Systèmes Simulia Corp., Providence, RI, USA website: https://www.sharcnet.ca/Software/Abaqus/6.14.2/v6.14/books/usi/default.htm

Sobhan, M. A. (2015). Concrete Highway Arch Bridges in Bangladesh : Historical Development and Lessons Learnt. *IABSE-JSCE Joint Conference on Advances in Bridge Engineering-III*, 978–984.

Tveit, P. (2006). *An Introduction to the Network Arch*.